

Chapter 2

The Response of EV Charging Loads to TOU Price

2.1 Introduction

One of the bottlenecks that restrict the rapid growth of EVs is the lack of the EV charging facilities [1–5]. The model of fuel cell charger is established and a corresponding control strategy is proposed in [3]. A new concept of mobile charger and its optimal scheduling methods are presented in [4]. With incremental development in EV charging facilities, EV loads are expected to increase phenomenally in the near future, which will bring negative impacts on the stability of power grids [6]. EV loads are seldom taken into account in current practice of power system planning, which results in risks in system operations and management [7].

There are three main ways to enable EV-friendly access to power grid: (1) V2G; (2) the use of energy management equipments (such as energy management concentrator and distributed energy management boxes); (3) the mechanism of electricity pricing. The power electronic converter technology that enables V2G is discussed in [8–10]. Energy management equipments can be used to maintain the balance between demand and supply, thus giving a boost to the utilization of EVs. Local and global smart charging control strategies based on home energy control box are discussed in [11], and it is discovered that smart charging control strategy can reduce peak load and level the load curve. The plug-in hybrid electric vehicle (PHEV) management equipments are adopted to manage PHEVs in cities in [12]. The PHEV management equipments are able to determine the number of PHEVs connected to the grid according to power flow calculation. Based on Micro-Simulation, the capacity of PHEVs connected to power grid by introducing intelligent charging policy implemented in central and distributed locations is optimized. Autostromboxes and the Demand Side Management System are used to manage the charging load in [13]. A global optimization technique is presented to reduce the error between reference curve and the summarized load curve of all charging events. The electricity pricing mechanism serves as the stimulation and guide for power demand and consumption mode of customers. Customers will

respond to variable electricity prices, decide whether they prefer charging or discharging EVs, and actively adjust charging rate and time. Countries with mature electricity market environment have focused their research on this area. For instance, an EV charging model based on real-time price information is introduced in [14], while Ref. [15] optimizes the charging process by using the method of quadratic programming and considering the relationship between electricity price and load demand. The objective is to minimize charging cost and maximize discharging profit. Linear programming model is used to make response to the real-time price in [16].

Situations are totally different in countries where electricity market is fully regulated. China's electricity market may be a typical example of regulated market, where electricity prices are decided by the government and, once enacted, remain unchanged for a relatively long time. At present, the electricity pricing mechanism in China mainly includes the catalog price, the stepwise power tariff and the TOU price. Unlike the catalog price and the stepwise power tariff, TOU price is not the same in different periods of one day, making it an important method for demand side management [17]. It is estimated that by 2050 the number of EVs in China will reach 200 million, and the total charging load will be up to 330 million kW [18]. With such a considerable capability, the EVs in China will play a significant role in balancing power supply and demand. Thereby, research on intelligent response to TOU price is of significance in market-regulated countries. Based on the existing research and the SOC curve, this chapter proposes an optimized charging model for a regulated market. By using the proposed method, EVs are able to adjust charging power and time and reduce the cost of customers, thus achieving peak shaving and valley filling in load demand.

2.2 Optimized Charging Model in Response to TOU Price

In regulated electricity markets, TOU price is set by the government in advance, and the prices remain unchanged for a long time. The user can set the expected ending time of charging when EVs are connected to the grid through the charger. To protect the battery from being damaged in charging process, the maximum charging power can also be set artificially. The charger with embedded TOU price module can intelligently formulate optimized charging scheme in consideration of the SOC curve and the maximum charging power set by the user, the aim of which is to minimize the cost and realize peak shaving and valley filling.

Objective Function. Take the cost that EV users need to pay to charge once as objective function

$$\min C = \int_{t_0}^{t_0+T} M(t)P(t)dt \quad (2.1)$$

In (2.1), t_0 is the starting time of charging, T is the duration of charging, $t_0 + T$ is the ending time of charging. $M(t)$ and $P(t)$ represent the unit price and charging power in time t respectively.

Constraints. The initial SOC of various EV batteries are different as driving modes and charging habits of different EV users are not the same. The energy demand of EV users with initial SOC considered is stated as below

$$\int_{t_0}^{t_0+T} P(t)dt = (1 - S_{ini})Q_r \quad (2.2)$$

In (2.2), S_{ini} represents the initial SOC of EV battery and Q_r is the rated capacity of EV battery.

According to Mass Theory [19], in order to reduce the life loss of EV battery, the charging current should not exceed the acceptable charging current of EV battery $I = I_0 e^{-\alpha t}$ (I_0 is the maximum charging current at the starting time, α is ratio of acceptance). Theoretically I_0 is determined by initial SOC and internal resistance of EV battery [20]. The highest acceptable voltage of EV battery should not exceed a certain limited value as well.

From the power expression $P = VI$, the charging power of EV battery should not exceed a certain limited value. The charging power is constrained by (2.3)

$$0 \leq P \leq P_{battery}(t) \quad (2.3)$$

In (2.3), $P_{battery}(t)$ represents the maximum acceptable charging power of EV battery in time t , which is the function of SOC and temperature of battery. Temperature effect on $P_{battery}(t)$ can be ignored when some measures are taken to keep the temperature of battery constant. Then the maximum acceptable charging power can be expressed as below

$$P_{battery}(t) = f(S) \quad (2.4)$$

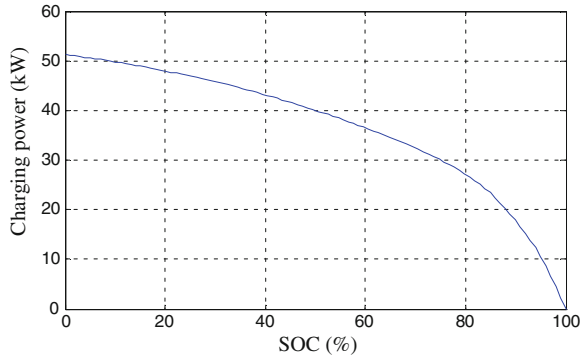
In (2.4), S is the current SOC of EV battery. The quantitative relationship between $P_{battery}(t)$ and S can be described by SOC curve which is shown in Fig. 2.1 [21].

Besides the constraint $P_{battery}$, which is the maximum acceptable charging power of EV battery, the maximum charging power is also restricted by: (1) the maximum power P_{user} set by EV users; (2) the maximum power $P_{charger}$ EV charger can output. Therefore, the actual maximum power in charging process is

$$P_{\max} = \min\{P_{user}, P_{charger}, P_{battery}\} \quad (2.5)$$

Usually, both the maximum power P_{user} set by EV users and the maximum power $P_{charger}$ EV charger can output are greater than the maximum acceptable charging power $P_{battery}$ of EV battery. So the actual maximum charging power P_{\max} is limited by $P_{battery}$ in most cases. Equations (2.2)–(2.5) consist of all constraints of optimized model presented above.

Fig. 2.1 The SOC curve.
 © (2012) IEEE. Reprinted,
 with permission, from
 Ref. [22]



2.3 Algorithm

As a continuous mathematical model, the above optimized model is discretized for the convenience of calculation. The total charging time T is divided into N periods, and the length of each period is Δt . The discretized optimized model can be expressed as:

$$\min C = \sum_{i=1}^N M(t_i)P(t_i)\Delta t \quad (2.6)$$

The constraint of maximum charging power limited by SOC is nonlinear, so a heuristic algorithm is designed [22].

- (1) Charge the EV battery with the maximum power P_{\max} from the starting time ($t = t_1$) until the battery SOC = 1 or $t = t_N$ (user-specified end time). If the battery is not filled until $t = t_N$, stop the optimization. Otherwise, go to step (2).
- (2) An initial feasible solution $P_0 = [p_1, p_2, \dots, p_n]$ (p represents the charging power) is obtained after step (1). Sorting the N periods based on TOU price is required. Symbols i and j are ascending sorted sequences, which means $M(t_i + 1) > M(t_i)$ and $M(t_j + 1) > M(t_j)$, $i = 1, 2, \dots, N$, $j = 1, 2, \dots, N$.
- (3) Set charge energy q as optimal step. The charge energy q transferred from high-price period to low-price period is defined as optimal step. The charge power e transferred from high-price period to low-price period can be expressed as $e = q/\Delta t$. In order to improve the precision of the simulation, q should take a small value such as 10^{-6} .
- (4) Assign $i = N$.
- (5) Assign $j = 1$.
- (6) Judge whether the energy left in period t_i is available for transference. When $P(t_i) > e$, go to step (7); otherwise, go to step (11).

- (7) Judge the sequence of period t_i and period t_j . If $t_i < t_j$, go to step (8), which means it will not break the SOC constraint when transferring energy q from period t_i to period t_j directly. The reason is as follows: Assume $Q(t_n)$ and $Q(t'_n)$ indicate the energy stored in battery before and after the transference respectively. When $n < j$, there exists $Q(t'_n) = Q(t_n)(n < i)$ or $Q(t'_n) = Q(t_n) - q (n \geq i)$; when $n = j$, there exists $Q(t'_n) = Q(t_n)$. It can be seen clearly that the SOC of EV battery in each period will not increase. As the charging power doesn't exceed the limit before the transference, the charging power cannot exceed the limit after the transference either. If $t_i > t_j$, go to step (9).
- (8) Transfer the energy from the high-price period to the low-price period. It can be expressed with mathematical equations as: $P(t_i) = P(t_i) - e$; $P(t_j) = P(t_j) + e$. After this, the procedure goes to step (6).

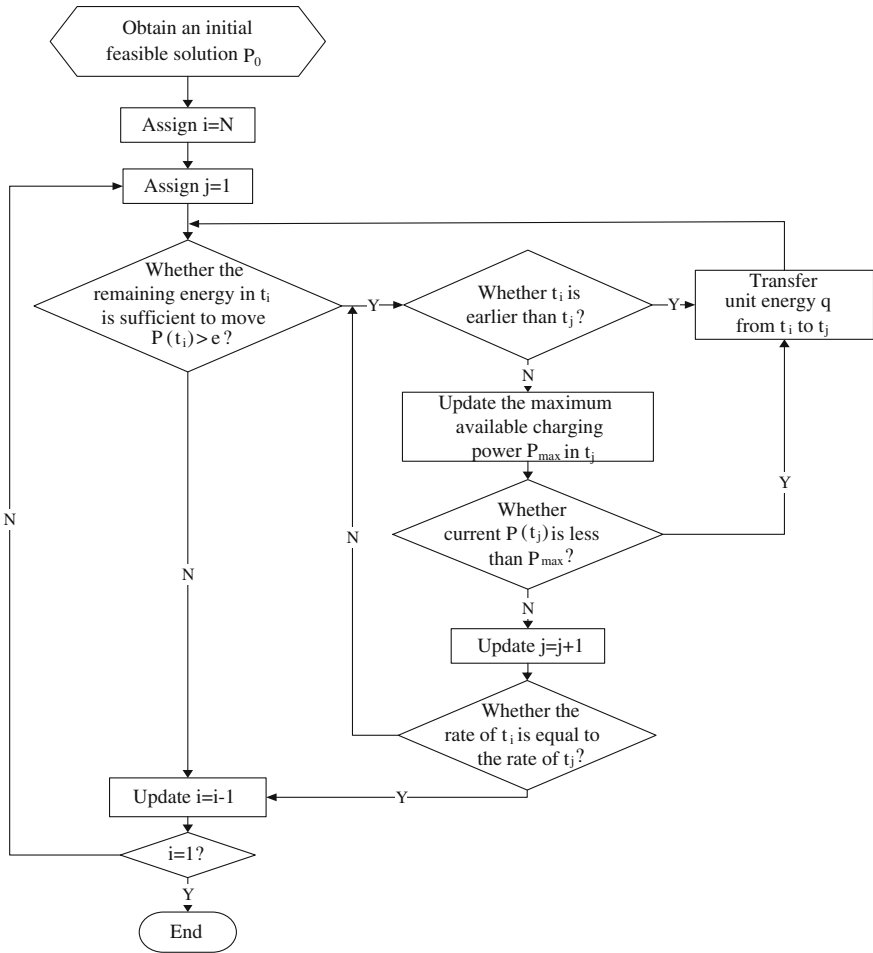


Fig. 2.2 The flowchart of optimization charge. © (2012) IEEE. Reprinted, with permission, from Ref. [22]

- (9) Judge whether $P(t_j)$ is sufficient to achieve the maximum charging power P_{\max} . If $P(t_j) < P_{\max}$, go to step (8); otherwise, go to step (10).
- (10) Set $j = j + 1$ and judge whether the price of period t_j is equal to the price of period t_i . If $M(t_i) = M(t_j)$, go to step (11); Otherwise, go to step (7).
- (11) Set $i = i - 1$ and judge whether i is equal to 1. When $i = 1$, it means there is no more energy that can be transferred from the high-price period to the low-price period, then stop the optimization. Otherwise, go to step (5).

The flowchart of the above optimization program is shown in Fig. 2.2.

2.4 Case Study

In order to verify the effectiveness of the optimized charging model presented in this chapter, a typical charging pattern for comparison is adopted. It is a common charging pattern of “plug and charge”, the charging profile of which is consistent with the charging characteristics of battery. Nevertheless, the charging profile may not follow the charging characteristics of battery in the optimized charging pattern, as it is determined by optimized charging algorithm which has been stated in previous section of this chapter. The charging cost and energy demand in different time are compared separately in two cases: single EV and multi-EV. In multi-EV case, the diversity of initial SOC and the starting charging time of different EVs should be considered. A probability model is introduced to describe the diversity, which will be discussed later. For single EV case, the randomness of initial SOC and the starting time of charging are neglected and assigned with specified value so as to get determined results, which is beneficial for us to understand the optimized charging model. In the following section, settings and results of simulation will be presented.

2.4.1 Settings of Simulation

Typical charging characteristics of lithium-ion battery. The charging curve of the lithium-ion battery equipped in Nissan Altra EV is shown in Fig. 2.3 [23]. In completely discharging situations, the demand for energy is 29.07 kWh. In this study, the charging curve in Fig. 2.3 of typical charging pattern is employed.

The starting time of charging. It has much randomness at the starting time of charging. And a distribution model of the starting time is established to describe this randomness. Assume that the distribution of the starting time obeys a Gaussian distribution, that is

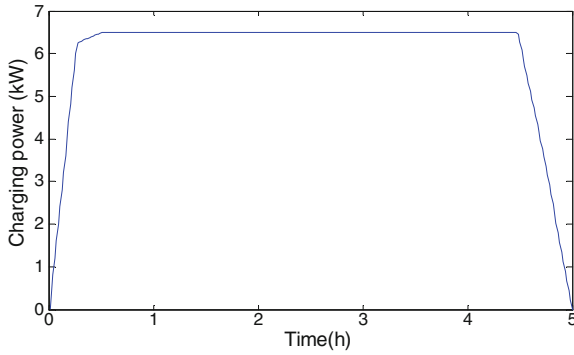


Fig. 2.3 The charging curve of the lithium-ion battery equipped in Nissan Altra EV. © (2012) IEEE. Reprinted, with permission, from Ref. [22]

$$f(t, \mu, \sigma) = \frac{1}{\sqrt{2\pi\sigma^2}} e^{-(t-\mu)^2/(2\sigma^2)} \tag{2.7}$$

Most EV users start charging after returning home from work at 18:00 and the starting time for charging of more than ninety percent of EV users is between 13:00 and 23:00. Therefore, in this case, it takes μ as 18 and takes σ as 5 [16]. The probability distribution of the starting time is shown in Fig. 2.4.

The initial SOC. The initial SOC of EV battery also presents some certain randomness. Using probability distribution model, it is described as

$$f(s, \mu, \sigma) = \frac{1}{\sqrt{2\pi\sigma^2}} e^{-(s-\mu)^2/(2\sigma^2)} \tag{2.8}$$

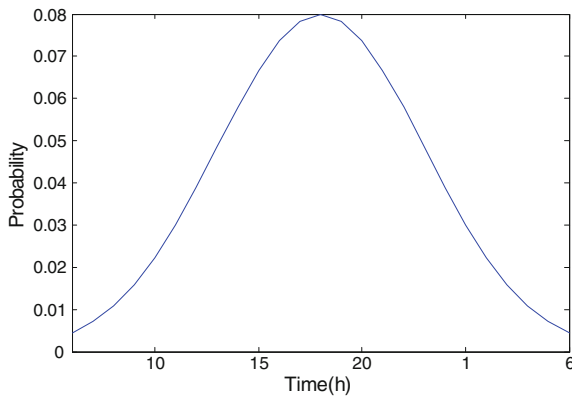
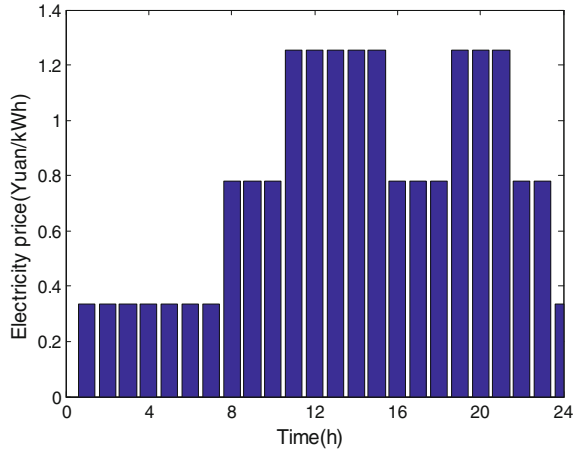


Fig. 2.4 The distribution curve of the starting time of charging. © (2012) IEEE. Reprinted, with permission, from Ref. [22]

Fig. 2.5 The histogram of TOU price. © (2012) IEEE. Reprinted, with permission, from Ref. [22]



s represents the initial SOC of EV battery and it is commonly between 0.2 and 0.8. It takes μ as 0.5 and takes σ as 0.3. μ is the average value of SOC and σ is the standard deviation.

TOU price. According to the actual TOU price implemented in Beijing, the period of valley load is defined as 23:00–07:00, totally 8 h; the period of peak load is defined as 10:00–15:00 and 18:00–21:00, totally 8 h. The remaining time is the period of flat load. Adopting the actual price of electricity in the city, the prices of peak, flat and valley load period are 1.253, 0.781 and 0.335 Yuan/kWh. The histogram of TOU price is shown in Fig. 2.5.

2.4.2 The Results and Analysis of Simulation

(1) The case of charging for single EV

In order to verify the effectiveness of the optimized charging model and for the convenience to observe the optimization process, the case of charging for single EV is implemented. Taking 20:00 as the starting time of charging and 12 h as the total charging time, the energy demand of typical charging pattern and optimized charging pattern in different time is shown in Fig. 2.6. As it can be seen, the optimized charging pattern can avoid peak demands and choose intelligently to charge in the time of valley demands, which can reduce charging costs.

(2) The case of charging for multi-EV

The starting time of charging and initial SOC should be considered in the case of charging for multi-EV. Therefore, the Gaussian distribution function is implemented to describe the differences. According to data of 2010, the number of automobiles in Beijing reached 4.69 million [24]. Assume the penetration of EVs (defined as the ratio of the number of EVs and the total

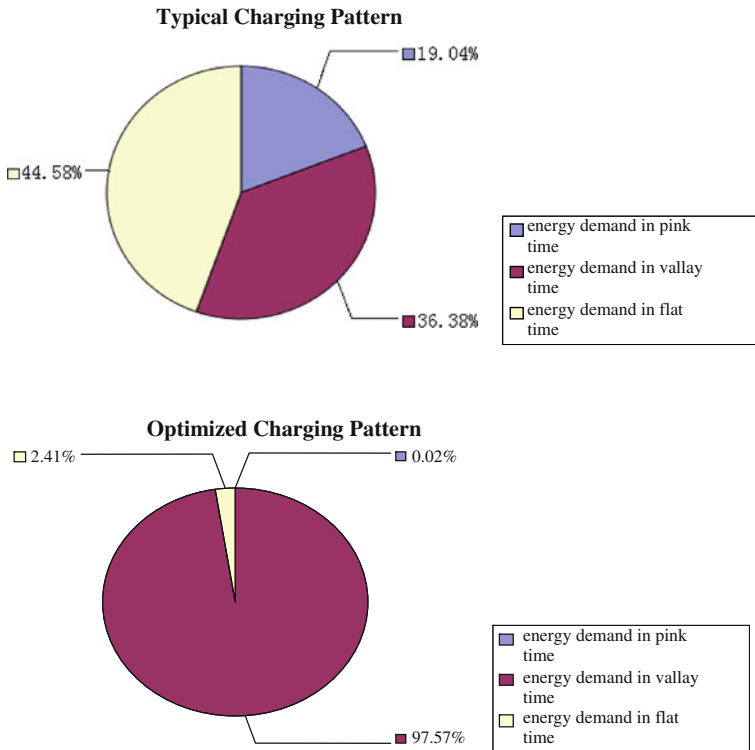


Fig. 2.6 The comparison of different charging patterns for single EV. © (2012) IEEE. Reprinted, with permission, from Ref. [22]

number of automobiles [11]) is 5 % and the number of EVs is about 234,500. In the process of computation, the average charging time of EV is about six hours. Figure 2.7 shows the energy demand of different charging patterns in Multi-EV charging case. As it can be seen, the optimized charging pattern in Multi-EV charging case can shift a mass of peak load to valley load, which is similar with that of single charging case.

Table 2.1 lists the charging cost of different charging patterns in different cases. It is clearly seen that the optimized charging pattern can bring a significant reduction in the charging cost of EV users. And it is evident that the performance of single EV case shown in the table is better than that of multi-EV case. The reason may be attributed to the available optimal space. In single EV case, the time span of charging covers more low-price periods, which means the optimal space and it is relatively large. So, through the optimization, almost all of the charging will be concentrated in low-price periods resulting in a better performance. From another perspective, it is implied that the charging cost will be less if EV users can consciously arrange appropriate plug-in time.

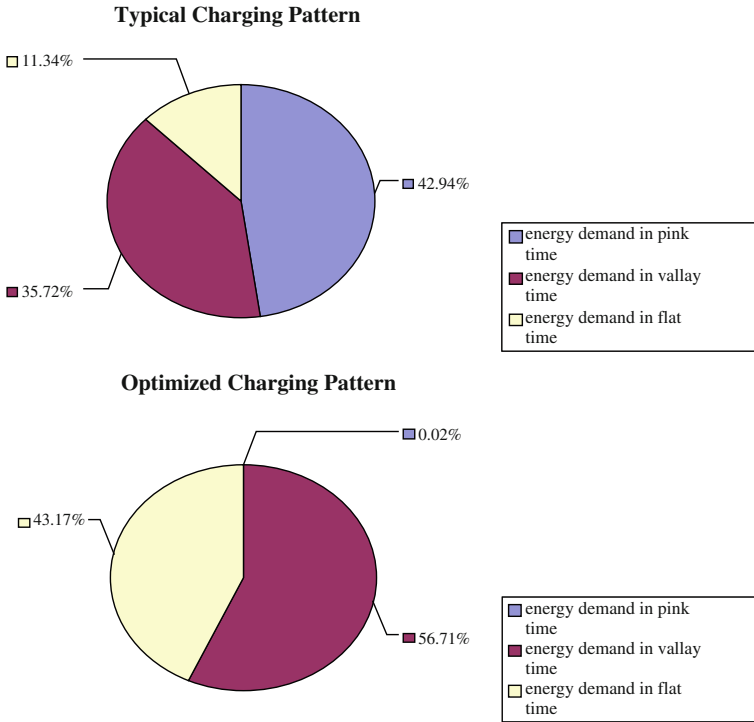


Fig. 2.7 The comparison of different charging patterns for multi-EV. © (2012) IEEE. Reprinted, with permission, from Ref. [22]

Table 2.1 The charging cost of different charging patterns in different cases

	Typical charging pattern	Optimized charging pattern	Reduction in cost (%)
The charging cost of single EV (Yuan)	20.673	10.02	51.52
The charging cost of multi-EV (104 × Yuan)	2179.4	1314.9	39.67

© (2012) IEEE. Reprinted, with permission, from Ref. [22]

2.5 Conclusions

In this chapter an intelligent charging method for EV charging facilities is proposed in response to TOU price. The purpose is to alleviate the stress in power grid under peak demand and to meet requirements for the demand response in regulated markets.

A comparative analysis of typical charging pattern and optimized charging pattern for charging performance in different cases is also presented. Simulation

results of both single EV and multi-EV have validated the effectiveness of the proposed approach. This chapter can serve as a useful reference for research on charging strategies in an open electricity market.

References

1. Etezadi-Amoli M, Choma K, Stefani J. Rapid-charge electric-vehicle stations. *IEEE Trans Power Del.* 2010;25(3):1883–7.
2. Takagi M, Iwafune Y, Yamamoto H, et al. Energy storage of PV using batteries of battery switch stations. *Proceedings of IEEE International Symposium Industrial Electronics (ISIE)* 2010;3413–3419.
3. Jiang Z, Dougal R. Control strategies for active power sharing in a fuel-cell-powered battery-charging station. *IEEE Trans Ind Appl.* 2004;40(3):917–24.
4. Li Z, Sahinoglu Z, Tao Z, et al. Electric vehicles network with nomadic portable charging stations. *Proceedings of IEEE 72nd Vehicular Technology Conference Fall (VTC 2010-Fall)* 2010;1–5.
5. Zhu X, Chen W, Luo J. Design and exploitation of supervisory control system for commercial electric vehicle charging station based on virtual DPU technology. *Proceedings of 2010 Power System Technology* 2010;1–5.
6. Salihi JT. Energy requirements for electric cars and their impact on electric generation and distribution systems. *IEEE Trans Ind Appl* 1973;IA-9(5):516–531.
7. Kabisch S, Schmitt A, Winter M, et al. Interconnections and communications of electric vehicles and smart grids. *Proceedings of IEEE Smart Grid Communications Conference* 2010;61–166.
8. Zhou X, Wang G, Lukic S et al. Multifunction bi-directional battery charger for plug-in hybrid electric vehicle application. *Proceedings of IEEE Energy Conversion Congress Exposition* 2009;3930–3936.
9. Pillai JR, Bak-Jensen B. Vehicle-to-grid for islanded power system operation in Bornholm. *Proceedings of IEEE Power Energy Society General Meeting* 2010;1–8.
10. Kisacikoglu MC, Ozpineci B, Tolbert L M. Examination of a PHEV bidirectional charger system for V2G reactive power compensation. *Proceedings of 25th Annual IEEE Application Power Electronics Conference Exposition (APEC)* 2010;458–465.
11. Mets K, Verschueren T, Haerick W, et al. Optimizing smart energy control strategies for plug-in hybrid electric vehicle charging. *Proceedings of IEEE/IFIP Network Operation and Management Symposium Workshops (NOMS)* 2010;293–299.
12. Rashid A, Waraichs D. Plug-in hybrid electric vehicles and smart grid: Investigations based on a micro-simulation. *ETH, Eidgenössische Technische Hochschule Zürich, IVT, Institut für Verkehrsplanung und Transport systeme* 2009;1–23.
13. Westermann D, Agsten M, Schlegel S. Empirical BEV model for power flow analysis and demand side management purposes. *Modern Electric Power System* 2010, Wroclaw, Poland. <http://www.meps10.pwr.wroc.pl/submission/data/papers/12.6.pdf>.
14. Markel T, Kuss M, Denholm P. Communication and control of electric drive vehicles supporting renewable. *Proceedings of IEEE Vehicle Power Propulsion Conference* 2009;27–34.
15. Shrestha GB, Chew BC. Study on the optimization of charge discharge cycle of electric vehicle batteries in the context of Singapore. *Proceedings of AUPEC Conference* 2007;1–7.
16. Qian K, Zhou C, Allan M, et al. Modeling of load demand due to EV battery charging in distribution systems. *IEEE Trans Power Syst* 2010;1–9.
17. Wang B, Li Y, Gao C. Demand side management outlook under smart grid infrastructure. *Autom Electric Power Syst.* 2009;33(20):17–22.

18. Xiao L, Lin L. Construction of unified new-energy based power grid and promotion of China's smart grid. *Adv Technol Electr Eng Energy*. 2009;28(4):54–9.
19. Yang Y, Lin Z, Qin D, et al. Control strategy and simulation study on NiMH battery quick charging for regenerative braking of HEV. *J Chongqing Univ*. 2007;30(3):1–5.
20. Meissner E, Richter G. Battery monitoring and electrical energy management precondition for future vehicle electric power systems. *Power Sources*. 2003;116(1–2):79–98.
21. Nelson RF. Power requirements for batteries in hybrid electric vehicles. *Power Source*. 2000;91(1):2–26.
22. Cao YJ, Tang SW, Li CB, et al. An optimized EV charging model considering TOU price and SOC curve. *IEEE Trans Smart Grid*. 2012;3(1):388–93.
23. Madrid C, Argueta J, Smith J. Performance characterization-1999 Nissan Altra-EV with lithium-ion battery. Southern California EDISON; 1999.
24. Qi Q, Yang Z. Vehicle population in Beijing over 4.69 million and drivers over 6.2 million. 2010. <http://auto.qq.com/a/20101201/000110.htm>.



<http://www.springer.com/978-3-662-49362-5>

Influences of Electric Vehicles on Power System and Key
Technologies of Vehicle-to-Grid

Li, C.; Cao, Y.; Kuang, Y.; Zhou, B.

2016, XV, 105 p. 46 illus., 18 illus. in color., Hardcover

ISBN: 978-3-662-49362-5